

Optical Manipulation of Defects in a Lyotropic Lamellar Phase

Yasutaka Iwashita and Hajime Tanaka*

Institute of Industrial Science, University of Tokyo, Meguro-ku, Tokyo 153-8505, Japan

(Received 19 August 2002; published 28 January 2003)

Here we study the line defect in a hyperswollen lamellar phase of lyotropic liquid crystal by applying a laser trapping method. We have succeeded in directly measuring the tension of a single isolated line defect and the adhesion energy between two defects. We demonstrate a new possibility of intentional patterning of various defects by direct optical manipulation. Furthermore, local rheological measurements provide information on the membrane organization around a particle and also evidence suggesting that flow in a lamellar phase has a two-dimensional nature.

DOI: 10.1103/PhysRevLett.90.045501

PACS numbers: 61.30.St, 87.80.Cc, 61.30.Jf, 82.70.Uv

Topological defect is a generic feature of the ordered state with broken continuous symmetry and is spontaneously formed upon ordering [1]. Clarifying the physical properties of defects is crucial for the basic understanding of the mechanical properties of an ordered phase. Since the elastic modulus of material, G , is related to the characteristic length scale of structural order, l , as $G \propto l^{-D}$ (D : dimensionality of the order), an ordered structure in soft matter composed of a mesoscopic unit has considerably lower elasticity than metals and semiconductors [2]. This feature of soft matter provides us with an ideal situation to study the structural, mechanical, and dynamic properties of a single defect. The low elasticity and the large characteristic size allow us, respectively, to manipulate a defect structure itself by using a weak external force (\sim pN) and to directly observe its dynamic response in real time with optical microscopy. It is known that defects sometimes weaken the mechanical strength of material, but this fact can positively be used to control the mechanical properties by introducing defects intentionally [3]. In this Letter, we study the physical properties of a single line defect [4] in a hyperswollen lamellar structure and spatially organize it by direct optical manipulation.

The samples we used are an aqueous solution of $C_{12}E_5$ (penta-ethyleneglycol mono n -dodecyl ether) and of $C_{10}E_3$ (triethyleneglycol mono n -decyl ether). Both $C_{12}E_5$ and $C_{10}E_3$ are nonionic surfactants. They are known to form various internal structures such as lamellar (L_α) and sponge (L_3) organization [2] made of surfactant bilayer membranes, depending upon the concentration ϕ and the temperature T [5,6]. Their characteristic length scales can be changed from nano- to micrometer just by changing ϕ , which is the concentration of surfactant in the solution. ϕ is ranged from 3 to 20 wt% in our experiments. The sample was confined between two parallel glass plates separated by about 50 μ m. We first heated a sample to transform it into the homogeneous sponge phase and then slowly cooled it down. The lamellar phase is nucleated and grows on the glass surface and eventually forms a uniform homeotropically aligned lamellar phase [7,8]. The perfect alignment of such a thick sample is possible

due to large intermembrane spacing d . Note that the strength of spatial confinement is characterized by d/L , where L is the length scale of the confinement. We put hydrophilic glass beads, whose radius a is 1.0 μ m, into the surfactant solution to create and manipulate line defects with optical tweezers. This provides us with an interesting situation of $2a/d \cong 10$ –100, depending upon ϕ . For a usual thermotropic smectic phase, this probe size should correspond to on the order of nm. This is a great advantage of using ordered soft matter with a larger characteristic length scale.

We apply a laser trapping method [9,10] for measuring the mechanical properties of a single line defect. We controlled the position of a laser spot (wavelength: 832 nm) focused by objective lens ($\times 100$, NA = 1.25) on a focal plane with the spatial resolution of 0.1 μ m, using two computer-controlled galvano mirrors. The motion of beads and defects were monitored by video-enhanced microscopy.

First we describe the characteristic features of a single line defect formed in the lamellar phase. When we disperse glass beads in a hyperswollen lamellar phase, most of them are localized either on line defects [3,11] or around other types of defects such as a multilamellar vesicle to lower the elastic energy [12], while some are dispersed as isolated beads. If we capture one of the glass beads trapped on such defects and pull it from the original position by the laser tweezers, a line defect is newly formed as a trace of the bead, as shown in Fig. 1(a). Note that the bead moves exactly on a two-dimensional plane in the lamellar structure. This is because we can never break up membranes by the force exerted on a bead by optical trapping (< 30 pN), and thus we are unable to move the bead vertically across membranes. Thus, the manipulation in a lamellar phase should be called “2D optical manipulation.”

The cross-sectional view of the line defect formed in this way and the defect structure around a bead at its end are schematically shown in Figs. 1(b) and 1(c), respectively [13]. Note that the number of membranes forming a defect should be even [for example, it is six for Fig. 1(b)] and exactly equal between both sides of the line defect.

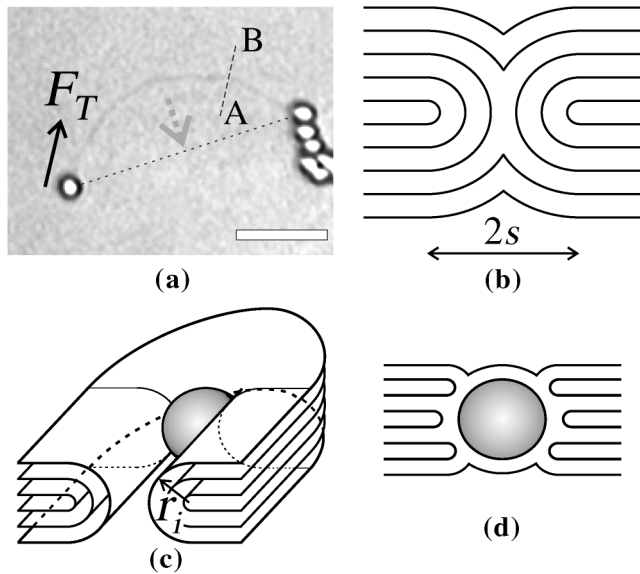


FIG. 1. A line defect and its structure. (a) A curved line defect formed by a glass bead ($a = 1 \mu\text{m}$) at 60.0°C for $\phi = 3.0 \text{ wt}\%$ C_{12}E_5 . The scale bar corresponds to $10 \mu\text{m}$. (b) Schematic defect structure, which corresponds to the A - B cross section in (a). The distance between the two singular lines which are the center of curvature radii r_i [see (c)] of cylindrically packed membranes is $2s$. We call it the line defect width or diameter. As directly observed in (a), $2s \approx 1 \mu\text{m}$ for $\phi = 3.0 \text{ wt}\%$. (c) Membrane structure around a glass bead located at the end of a line defect. (d) Membrane structure around an isolated glass bead (not on a line defect).

This constraint stems from the connectivity requirement for membranes, which must be very strictly satisfied. The bead at the end of a line defect is surrounded by a half line defect of width s , or located in a passagelike point defect [3,14]. This is revealed from the following fact. If we release the bead after moving it, it returns to the original position, following the shrinking line defect on its path. This shrinking process can be regarded as the repairing process of a line defect, where the transformation from folded to planar membranes keeps occurring around the bead. Note that there is no change in the topology. Defects are neither created nor annihilated during this process.

We can create a curved line defect by moving a bead quickly on a curved path [15], as shown in Fig. 1(a). Then, if we keep the bead at a fixed point, the defect gradually becomes straight (as indicated by a dashed line) to minimize the length of the line defect. Since this relaxation speed of the curvature is much slower ($\sim 10 \text{ s}$) than the speed of defect repairing, which is determined from the velocity of the bead (for example, $v \sim 10 \mu\text{m/s}$ for $\phi = 0.03$), the released bead returns on the curved path created. Thus, the bead can record its path, or the history of its motion. If we draw a spiral pattern, for example, and release the bead by switching off the laser power, the bead just follows the spiral path. This interesting behavior

strongly supports the above interpretation that the defect shrinking is the repairing process of the line defect itself.

By applying laser tweezers, we have succeeded in directly measuring the line tension of a single line defect, F_T , by balancing it with a trapping force of a bead at the end of the line defect. We measure the minimum trapping force, below which the bead is released and the defect starts to shrink, which should be equal to the line tension F_T . The ϕ dependence of F_T for C_{12}E_5 solutions is shown in Fig. 2.

We also theoretically estimate the line tension by assuming the defect structure shown in Fig. 1(b). Here the energy associated with the singular part in Fig. 1(b) is neglected since such singularity would be avoided in a real system [13]. Then, the line tension, which is the total excess curvature energy per unit length of a line defect, can straightforwardly be calculated as

$$F_T = \sum_{i=1}^m \frac{\pi\kappa}{r_i} + \sum_{i=m+1}^{\infty} \frac{2\kappa}{r_i} \sin^{-1} \frac{s}{r_i}, \quad (1)$$

where $r_i = [1/2 + (i-1)]d$ ($i = 1, 2, 3, \dots$) and κ is the membrane's curvature elastic modulus. Here m is the number of folded membranes [e.g., $m = 3$ in Fig. 1(b)], and thus it should be an integer close to $s/d \sim a/d$ for our case. The first term of the right-hand side of Eq. (1) represents the energy associated with the folded part, the second term the energy associated with the unfolded part. Since $d \approx \delta/\phi$, where δ is the thickness of a bilayer membrane, and $\delta \approx 3.75 \text{ nm}$ for our system [5], m should be about 8, for example, for $a = 1 \mu\text{m}$ and $\phi = 0.03$. The width of a defect, $2s$, should be comparable to a . The line tension measured agrees well with this theoretical prediction [Eq. (1)] with $\kappa = 0.95k_B T$ [16] (see Fig. 2) [17]. Note that there is no adjustable parameter.

Next we focus on the local rheological properties of a hyperswollen lamellar phase around a bead. The effective viscosity η_{def} for the motion of a bead at the end of a defect can be estimated from its velocity, v , since the

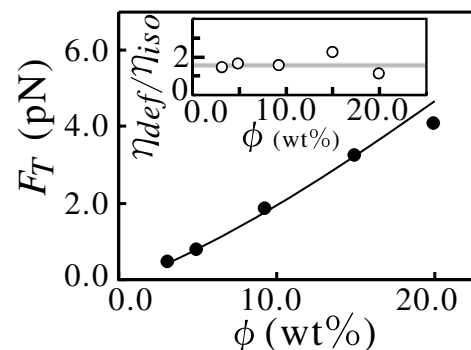


FIG. 2. The measured line defect tension (filled circles) for C_{12}E_5 solutions and the theoretical prediction (solid curve). Each data point is the average of data for about 10 different line defects. The inset plots $\eta_{\text{def}}/\eta_{\text{iso}}$ against ϕ . The gray line represents $\eta_{\text{def}}/\eta_{\text{iso}} = 1.6$.

viscous drag force F_v should be balanced with the tension F_T as $F_T = F_v = 6\pi\eta_{\text{def}}av$. We also make an independent measurement of the effective viscosity η_{iso} for the motion of a single isolated particle (not in a line defect): We measure the corresponding Stokes force ($F_v = 6\pi\eta_{\text{iso}}av$) from the minimum trapping force required for manipulating the particle with a constant speed v . We confirm the proportionality of F_v and v for both cases, indicating that the fluid behaves as a Newtonian fluid. However, we find that the η_{def} is larger than η_{iso} by a factor of $1.6 \cong (a + s)/a$ for all the surfactant concentrations (see the inset of Fig. 2). This suggests the difference in the defect structure between the two cases: A bead at the end of a line defect accompanies the passagelike defect structure (characteristic size s) around it [see Fig. 1(c)] upon its motion, while an isolated one may not accompany such a large defect structure. We speculate that the defect structure for the latter is the one composed of m membranes that are independently folded one by one [see Fig. 1(d)]. This defect structure has a higher energy than the large passagelike one where m membranes are folded together [see Fig. 1(c)], but it is favorable if we consider the process of defect formation upon the transformation of the sponge structure to the lamellar one around a particle and isolated particles are rather rare. Note that in the sponge phase an isolated bead is expected to be surrounded by folded parts of membranes that form a sponge structure. This example indicates that our method has the potential to provide interesting information on the local membrane organization around a bead, which is hardly obtained by other methods.

Here it is worth mentioning that our viscosity measurements described above, in particular, the proportionality between F_v and v , directly support the view that the medium is a fluid made of membranes and intermembrane liquid. For example, the surfactant molecules in a membrane should flow along it; otherwise, defects must be created on each membrane upon the motion of a bead, which would lead to breakdown of the proportionality between F_v and v . Furthermore, the 2D nature of flow in a lamellar phase is confirmed by the following fact. If we assume that a line defect whose width is $2s$ moves in a 3D fluid of viscosity η , then the friction force for the translational motion of a line defect per unit length is estimated in the Oseen approximation as $F_{\text{line}} = \frac{8\pi\eta v_{\text{line}}}{2A+1}$ by regarding the line defect as a cylinder with a radius of s . Here $A = \ln \frac{4\eta}{s\rho v_{\text{line}}} - \gamma$, where $\gamma = 0.5772$ is the Euler number and v_{line} is the translational velocity of a line defect. We experimentally confirmed that v_{line} measured is slower than that estimated by the above relation for a 3D fluid by about 1 order of magnitude. Note that they should be the same if the assumption made (the 3D nature of fluid) is correct. This discrepancy supports the quasi-2D nature of fluid in a lamellar phase (or low permeability of fluid across membranes).

Finally, we demonstrate the 2D patterning of line defects in a lamellar phase by using 2D optical manipulation of a bead. Two typical examples are shown in Figs. 3 and 4. One is the network of line defects (see Fig. 3). It behaves as a network of elastic strings, which can be used to control the elasticity of the system [3,11]. The other is a spiral pattern of a line defect [see Fig. 4(a)]. It should be noted that these 2D patterns need to satisfy the elastic force balance condition so that they are stable. For the former, the elastic force balance on the network of a line defect can be seen from the fact that three arms always make an angle of 120° at their junction point (see Fig. 3). For the latter, on the other hand, the spiral pattern is stabilized by the adhesion force between the neighboring line defects.

Let us consider the adhesion between line defects, which is a key physical factor for the formation of a spiral pattern having a constant spacing between neighboring line defects. Neighboring line defects should be made of the same number of membranes and exist exactly on the same height in a lamellar phase. Our observation tells us that they interact with each other when their distance becomes less than $1 \mu\text{m}$, which is our spatial resolution of microscopic observation. We experimentally estimate the adhesion energy from the condition for the spiral pattern to be stable, as follows. The line tension of the adhered line defect, F_7^a , should be balanced with the line

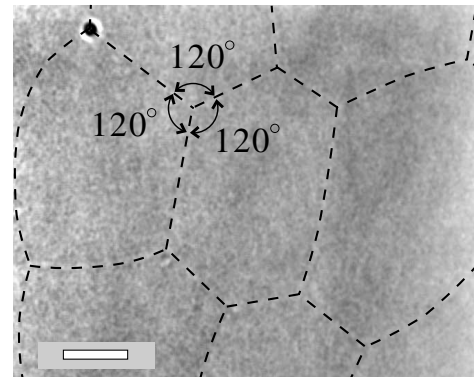


FIG. 3. Network of line defects formed by 2D optical manipulation at 35.0°C for the lamellar phase of a C_{10}E_3 solution ($\phi = 10.1 \text{ wt } \%$). The scale bar corresponds to $10 \mu\text{m}$. Dashed lines, which are to guide the eye, represent line defects. According to the model in Fig. 1, the region surrounded by a line defect should have a closed pancakelike membrane structure. It is similar to a uniaxially compressed multilamellar vesicle, whose thickness is equal to that of a line defect. If the line tension is balanced everywhere in the network structure, it is stable. If we violate this force balance, the network structure slowly shrinks and eventually disappears. The mechanism of shrinking of the pancakelike region may be an evaporation-condensation-like mechanism. Since exchange of surfactant molecules between membranes is very slow, such a closed region maintains its size for more than 10 min, supporting the above mechanism.

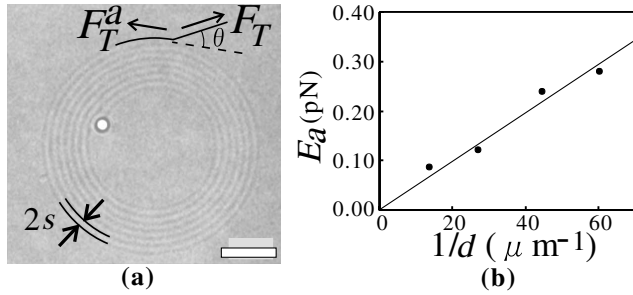


FIG. 4. (a) Optically manipulated 2D spiral pattern. It was observed at 60.0°C for $\phi = 9.2$ wt% C_{12}E_5 . The scale bar corresponds to $10\ \mu\text{m}$. Solid and dashed lines are to guide the eye. (b) The adhesion energy per unit length of line defect, E_a is plotted against $1/d$, which is proportional to ϕ . Each data point is an average of the results of five measurements. E_a is about 10% of the line tension.

tension of an isolated line defect, F_T , to have the angle of θ between them at a sharp kink [19] [see Fig. 4(a)]. Thus, we obtain the relation of $F_T^a = F_T \cos\theta$. From this, we can estimate the adhesion energy per unit length as $E_a = F_T - F_T^a$. In Fig. 4(b), the adhesion energy E_a estimated in this way is plotted as a function of $1/d$, which is proportional to ϕ , for C_{12}E_5 solutions. The result is consistent with a simple scaling prediction, $E_a \sim k_B T/d$, which is based on the fact that d is the only relevant length scale [18].

To summarize, we have revealed the physical properties of a single defect and the local rheological properties of a lamellar phase and successfully drawn 2D patterns by its optical manipulation. Our method may be applied to other types of topological defects of ordered soft matter.

This work was partly supported by a Grant-in-Aid for Scientific Research from the Ministry of Education, Culture, Sports, Science and Technology, Japan.

*To whom correspondence should be addressed.

- [1] P.M. Chaikin and T.C. Lubensky, *Principles of Condensed Matter Physics* (Cambridge University Press, Cambridge, 1995).
- [2] See, e.g., *Soft Matter Physics*, edited by M. Daoud and C. E. Williams (Springer, Berlin, 1999).
- [3] M. Zapotocky *et al.*, *Science* **283**, 209 (1999).
- [4] We call a linelike defect created by the motion of a bead a line defect, although, strictly speaking, it should be called, e.g., a defect loop.
- [5] R. Strey *et al.*, *J. Chem. Soc.* **86**, 2253 (1990).
- [6] H. Tanaka *et al.*, *Phys. Rev. Lett.* **89**, 168303 (2002).
- [7] P. Boltenhagen *et al.*, *J. Phys. II (France)* **1**, 1233 (1991).
- [8] C. Blanc *et al.*, *Eur. Phys. J. E* **4**, 241 (2001).
- [9] A. Ashkin, *Phys. Rev. Lett.* **24**, 156 (1970).
- [10] M. Miwa *et al.*, *Jpn. J. Appl. Phys.* **39**, 1930 (2000).
- [11] G. Basappa *et al.*, *Eur. Phys. J. B* **12**, 269 (1999).

- [12] P. Boltenhagen *et al.*, *Phys. Rev. A* **46**, R1743 (1992).
- [13] See, e.g., M. Kléman, *Points, Lines and Walls* (Wiley, Chichester, 1983).
- [14] L. Golubović, *Phys. Rev. E* **50**, R2419 (1994).
- [15] If we try to move a bead across the line defect formed by itself, we always fail. This is again because we can never break up membranes (or induce topological change of membranes) with our limited optical trapping power. Since the membranes between the bead and the line defect are on the same height, the motion of a bead across the line defect formed by itself inevitably requires the reorganization of membranes accompanying the topological change, which is energetically prohibited.
- [16] This value of κ was estimated by our independent experiment for the same system.
- [17] The agreement between the measured F_T and the theoretical prediction in Fig. 2 suggests the validity of our assumptions; for example, (i) the singular parts in Fig. 1(b) may be avoided without costing large elastic energy, and (ii) the resulting layer-compression energy is also considerably smaller than the bending one. This may be a unique feature of lyotropic smectics having an extra degree of freedom, concentration. Although the above assumptions may be valid for a single isolated line defect, the layer-compression energy is important when we consider the interaction between line defects (see [18]), and it may also play a significant role around the bead.
- [18] The mechanism behind this relation can be explained as follows. For the defect structure shown in Fig. 1(a), the distortion around the core region involves not only bending but also layer compression to minimize the total elastic energy [17]. The latter induces attractive interaction between two line defects, which leads to their adhesion, since overlap of the distortion fields lowers the energy associated with them. The characteristic length scale of the additional distortion should be the order of the penetration depth of the smectic order [1], λ , which is estimated as $\lambda = \sqrt{\kappa/Bd} \sim d$. Thus, the extra deformation should be localized in the length scale $\sim \lambda$, which is smaller than $2s$. Provided that the distortion field can be characterized by the only one length scale λ , the energy associated with the deformation, f_{dB} , should be proportional to the characteristic area of the deformation, $\lambda^2 \sim d^2$, and the layer-compression modulus [2], $B \sim d^{-3}$. Thus, we obtain the following scaling relation: $f_{dB} \propto B\lambda^2 \sim d^{-3}d^2 = d^{-1}$. Thus, the adhesion energy per unit length is estimated as $E_a \sim f_{dB} \propto d^{-1}$.
- [19] The rounding length, or the persistence length, ξ_r , of a line defect can be estimated as follows. It is known that $\xi_r^2 \sim (\kappa_l/F_T)$, where κ_l is the curvature elasticity of a line defect. Since the bending deformation of a line defect should cost less energy than the bending deformation of $2m$ membranes stacked in parallel with a spacing of d , whose thickness and width are both $2s$, we obtain the relation of $\kappa_l < 2m \times \kappa \times 2s$. By putting in reasonable parameters, we immediately conclude that $\xi_r < 0.5\ \mu\text{m}$, which is consistent with the observed sharp kink at the detached point of an adhered line defect [see Fig. 4(a)].